

Nuclear magnetic resonance imaging – a potential method for analysis of bone material

J. TIMONEN, L. ALVILA, P. HIRVA, T. T. PAKKANEN

University of Joensuu, Department of Chemistry, P.O. Box 111, FIN-80101 Joensuu, Finland
E-mail: jtimonen@joy1.joensuu.fi

The basic usage of nuclear magnetic resonance (NMR) microimaging for materials characterization is introduced. An application of microimaging for three-dimensional structural study of trabecular bone is presented with elementary types of image presentation. Solid bone in itself does not produce any significant NMR intensity and natural lipids and/or added 70% ethanol has been used as a signal source. The applied pulse sequences were three-dimensional spin echo and three-dimensional chemical shift selective spin echo. © 1998 Chapman & Hall

1. Introduction

The phenomenon of nuclear magnetic resonance (NMR) was first discovered in 1945 simultaneously by Bloch [1] and Purcell [2]. After evolution of super-conductive magnets and fast computers, NMR is nowadays one of the major analytical tools in chemistry. The idea of using NMR to gain spatial information, or an image, from a sample was demonstrated by Lauterbur in 1973 [3] and since then the clinical MR scanners have become a routine analysis method in clinical medicine. The basics of NMR imaging lie on the application of linear magnetic field gradients to sample space. Because the NMR frequency of a given nucleus depends on the magnetic field strength of the instrument, the variation of the field with an arbitrary coordinate creates a frequency–coordinate correlation. This simple correlation with selective radio frequency pulses makes it possible to produce two- or three-dimensional images of the presence of the NMR-nucleus involved [4, 5].

A simplified Fourier transform (FT)–NMR imaging process consists of a series of spin echo pulse sequences combined with space-encoding field gradients. The raw data, i.e. the collected echo signals, are further Fourier transformed to gain an image of the sample. Modern imaging equipments offer a variety of pulse sequences and a user can select a suitable one depending on the type of experiment. The collected signal, as in the usual NMR experiments, is a function of the quantity of the measured nucleus, i.e. spin density, and of the relaxation and diffusion processes involved. The contrast of the image can thus be made to reflect pure spin density or relaxation properties of nuclei in different regions of the sample. As these properties are characteristic of the physical status of the sample, the nuclear magnetic resonance imaging (NMRI) tool opens huge perspectives in the structural characterization of materials. Also, one significant point of view is the capability to produce chemical

shift selective images and thus track the distribution of a given chemical substance.

The major demands of NMR imaging on the sample are the size of the sample and the presence of an NMR-active nucleus with convenient relaxation properties. In NMR microscopy experiments, the standard coils have an access in the range of 2–12 mm. The nucleus measured should have a high natural abundance, in practice most of the work in this field is done with ^1H , although other abundant isotopes, mainly ^{31}P [6] and ^{19}F [7], can be used. The relaxation of the measured nucleus should be long enough to gain a sufficient echo signal, in the case of protons a natural linewidth below 2000 Hz should be measurable. Naturally, a sample containing large quantities of paramagnetic species is bound to cause problems. When the sample contains several intense NMR signals, the feasible image resolution becomes poorer and chemical shift selective methods are usually needed for true microscopy range experiments. An ideal imaging sample contains only one type of nucleus producing a single resonance line. In medical imaging, this criterion is readily more or less filled, whereas materials may need careful sample preparation. On the other hand, compared to clinical scanners, the NMR microscopy accessories are able to produce a much better image resolution, a three-dimensional image voxel of $(10\ \mu\text{m})^3$ is currently achievable.

Porous materials form a significant type of solid matter that finds use in many kinds of environments. Although routine NMR microscopy in solids is not yet a daily procedure, adding an appropriate liquid phase for imaging gives a possibility to study the solid structure. Applications in catalysts [8, 9], building materials [10] and stone [11] serve as an example of this field.

This paper presents some preliminary results of our project on NMR microscopy of the trabecular bone. In the presented images, usage of natural lipids or

added solvents to execute NMR microscopy is demonstrated. Diseases like osteoporosis are responsible for structural weakening of inorganic bone. This degradation of structure exposes the bone to fractures and reduces recovery. With suitable medication, the degradation of the trabecular bone can be cured to some extent [12]. NMR microscopy offers a non-destructive analysis method to study the characteristics of solid structure of bone material and changes in it due to sicknesses or medications.

2. Experimental procedure

The samples of bone material were the tibia of a rat stored in ethanol (A) and two fresh femurs (B,C) (provided from Leiras Ltd). The NMR imaging experiments were performed on a Bruker AMX-300 WB spectrometer operating at 300 MHz (^1H), equipped with a microimaging accessory and a 7 T vertical bore superconducting magnet. The measurements were carried out using spin echo three-dimensional pulse sequences.

The tibia sample (A) was fixed in 70% ethanol and imaging was performed in a vertical 5 mm r.f. coil in ethanol. In a typical experiment, TR was 1000 ms, TE 5 ms, field of view (FOV) $8 \times 8 \times 8 \text{ mm}^3$ with the $128 \times 128 \times 128$ matrix, which results in a resolution of $(62.5 \mu\text{m})^3$.

A fresh femur sample (B) with natural lipids, was placed in a 10 mm NMR tube without a solvent. The proton signal was picked up by a Helmholtz coil of 10 mm diameter. The images were recorded with a spin-echo time (TE) of 3.76 ms and a repetition time (TR) of 200 ms. The image comprised $256 \times 128 \times 128$ voxels (volume cells) and the FOV was $20 \times 10 \times 10 \text{ mm}^3$. The phase gradients were 9.44 G cm^{-1} and the read gradient 11.75 G cm^{-1} , which achieved a resolution of $(78.1 \mu\text{m})^3$.

In order to obtain bone images with a better resolution $(39.1 \mu\text{m})^3$, the femur (C) was cut, and a small amount of ethanol was added to reduce drying and to increase signal. The knee-joint was placed between two teflon plates in a 5 mm NMR tube. A microimaging probe was fitted with a 5 mm horizontal solenoid coil, where FOV was $5 \times 5 \times 5 \text{ mm}^3$. The image matrix size was $128 \times 128 \times 128$ data points, TE 2.88 ms, TR 200 ms, phase gradients 28.69 G cm^{-1} and the read gradient 46.98 G cm^{-1} .

3. Results and discussion

Spin-spin or transverse relaxation time constants, T_{2s} , of protons in solid bone material are too short and the signals are too broad for conventional NMR imaging methods, which means that bone itself gives no signal in NMR measurements. Line narrowing with magic-angle rotation and multipulse techniques can be applied to collect NMR signals from a rigid and solid sample matrix, but obtaining microscopic resolution is still difficult [13–15].

A simple indirect method to image the fine structure of a solid material is to allow a proton-containing solvent to penetrate into the sample and collect the

signal of the solvent. Naturally, NMR imaging is also an excellent technique for studying the diffusion of solvent into a solid material [16].

The tibia (A) of a rat was exposed to 70% ethanol/water mixture in order to obtain a spatially resolved NMR data. All signals from the frequency spectrum were incorporated in the echo signals by applying a large enough sweep width. A slice from the centre of a three-dimensional image is presented in Fig. 1, where the bone is seen in horizontal position. The uniform tubular bone is found as a black area of low intensity and the solvent gives the light area of high intensity. A clear channel-shaped fracture through the bone can be discovered in tibia on the lower side of the cross-section.

Fig. 1 also presents some typical artefacts of NMR images. Small changes in grey scale of solvent area are due to incomplete shimming, leading to slight inhomogeneities in magnetic field during the measurement. Similar artefacts are expected also in cases where the linearity of the field gradient is insufficient. Another typical artefact, a misty pixel line of higher intensity, about one-third of the figure width from the left frame, is seen in Fig. 1. This virtual intensity is caused by the geometry of Helmholtz coils and is located in the centre of FOV. Solenoid coils do not produce these errors. The two spherical areas with low intensity near the right frame are air bubbles.

Chemical shift selective imaging is a technique by which the spatial distribution of a particular species of frequency spectrum can be imaged [12]. Three-dimensional chemical shift imaging has been applied on the lipid signals of fresh femur samples B and C. Slices from the datasets are presented in Figs 2 and 3. The NMR image of the natural fats in the knee-joint of a rat femur (B) is seen in Fig. 2. The grey scale of the image has been inverted to highlight the solid bone with light area; respectively, the dark areas contain mobile protons, in this case lipids. The method seems to provide a contrast good enough to visualize details of a sample. However, in long three-dimensional measurements, added solvent or sample cooling is

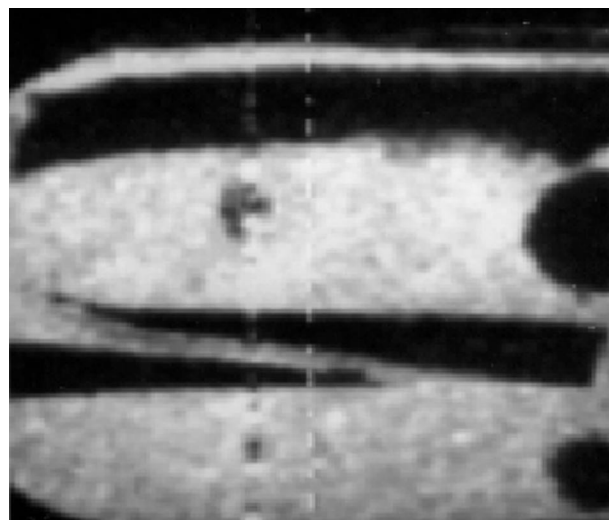


Figure 1 An NMR image of the tubular section of a rat tibia immersed in ethanol/water mixture.

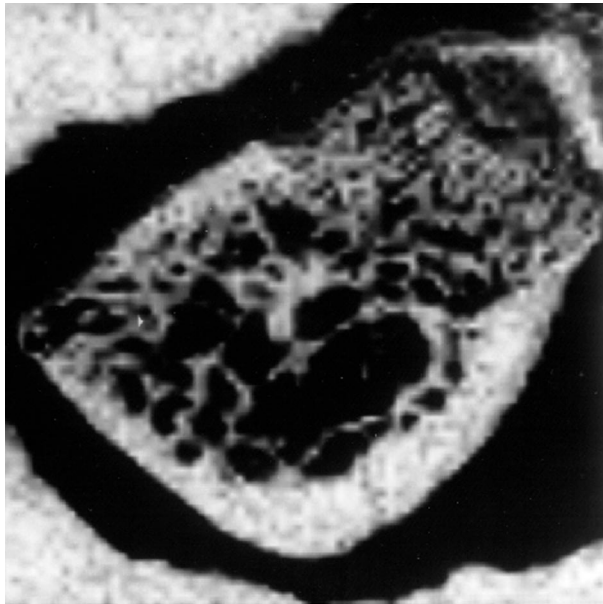


Figure 2 A slice from a three-dimensional chemical shift selective image of the natural fats of a femur knee joint. Voxel resolution $78.1 \mu\text{m}^3$.

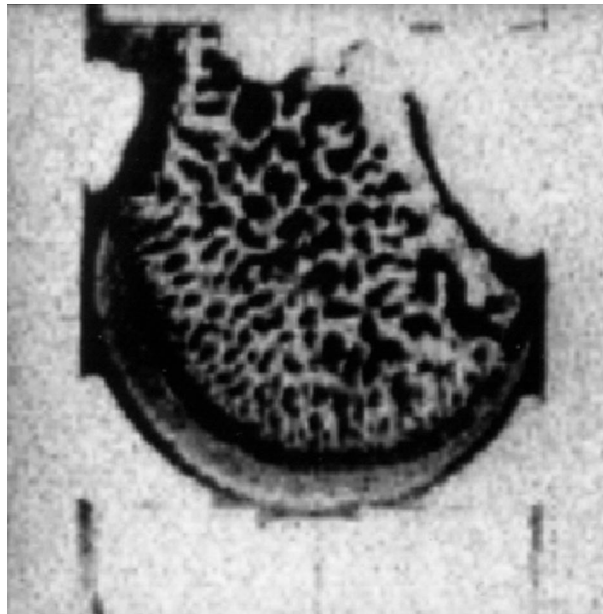


Figure 3 A slice from a three-dimensional chemical shift selective image of the natural fats of a femur knee joint. Voxel resolution $39.1 \mu\text{m}^3$.

needed to prevent drying, which results in reduced signal.

In order to obtain a better resolution and more exact structures, a specimen of a knee-joint from femur (C) was studied with three-dimensional chemical shift selective imaging and the grey scale of the image data was inverted to correspond to real bone structure (Fig. 3). With an image voxel size of $(39.1 \mu\text{m})^3$ the fine structure of the trabecular bone is quite clearly obtainable.

Surface reconstruction is a technique which creates a three-dimensional surface to a chosen intensity level of an image. In our case, the surface rendering was done for the dataset of Fig. 3, cutting out the

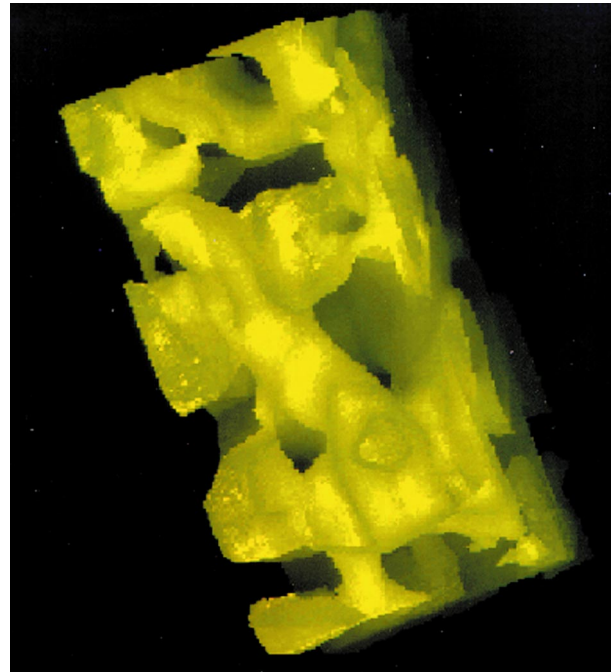


Figure 4 Three-dimensional surface reconstruction of the trabecular bone inside a knee joint.

volumes of any significant intensity. A selected part of the surface reconstruction image (Fig. 4) presents three-dimensional network of trabecular bone inside the joint. In degradative bone diseases, the mass of trabecular bone is usually decreased and the surface reconstruction offers a valuable tool for defining the real volume of solid bone in sample.

4. Conclusions

NMR microimaging, as an analysis method for the structural characterization of trabecular bone, is a promising non-degradative way to present true three-dimensional construction of an inorganic matrix. In fresh or living samples, chemical shift selective imaging provides a way to determine spatial distribution of given NMR signals, i.e. tissue water or lipids. In cases where fresh tissue is not available, or the mobile phase of the sample is not stable enough, added solvent can be applied to produce NMR intensity from void space. Three-dimensional spin echo pulse sequences are very time consuming; a faster alternative for cases where experimental time is a crucial factor are gradient echo pulse sequences with low-angle excitations [17]. In our case, sufficient sample stability was maintained with additional solvent.

The preliminary results presented in this paper demonstrate the capability and some typical artefacts of the technique. Both three-dimensional spin echo and three-dimensional chemical shift selective imaging sequences are able to visualize the structure. When more than one signal is present in the frequency spectrum, the chemical shift imaging produces images with better resolution. Chemical shift imaging of natural lipids is also a better choice if the solid structure can be damaged by drying or solvent. When the structure is stable, an additional solvent can remarkably intensify signal-to-noise ratio in an image. In these cases

better results are expected when the lipids and soft tissue are washed out and the solvent contains only one NMR signal. The obvious choice for solvent in these kinds of experiment is water.

The method is readily applicable in prosthetic medicine for studying three-dimensional microfractures and interfacial corrosion between prosthesis, bone cement and natural bone. Naturally, as the resolution within reach is dependent on the sample size, the major possibilities lie in the animal-test phase of product development.

Acknowledgements

The authors thank Dr Volker Lehmann and Dr Dieter Gross, Bruker Analytische Messtechnik, Rheinstetten, Germany, for very profitable collaboration.

References

1. F. W. BLOCH, W. W. HANSEN and M. PACKARD, *Phys. Rev. Lett.* **69** (1946) 127.
2. E. M. PURCELL, H. C. TORREY and R. V. POUND, *ibid.* **69** (1946) 37.
3. P. C. LAUTERBUR, *Nature* **242** (1973) 190.
4. P. T. CALLAGHAN, "Principles of Magnetic Resonance Imaging" (Clarendon Press, Oxford, 1991).
5. "Magnetic Resonance Microscopy" edited by B. Blümich and W. Kuhn, (VCH, Weinheim, 1992).

6. B. G. WINSBORROW, P. KOZLOWSKI, C. L. FILGUEIRAS, L. SHABNAVARD, J. YE, A. ARONOV, J. SCOTT, T. A. SALERNO, J. K. SAUNDERS and R. DESLAURIERS, *Can. J. Appl. Spec.* **39** (1994) 135.
7. S. N. SARKAR, J. J. DECHTER and R. A. KOMOROSKI, *J. Mag. Reson. A* **102** (1993) 314.
8. M. P. HOLLEWAND and L. F. GLADDEN, *J. Catal.* **144** (1993) 254.
9. J. TIMONEN, L. ALVILA, P. HIRVA, T. T. PAKKANEN, D. GROSS and V. LEHMANN, *Appl. Catal. A* **129** (1995) 117.
10. L. PEL, PhD Thesis, Technische Universiteit Eindhoven, The Netherlands (1995).
11. S. BOBROFF, G. GUILLOT, C. RIVIÈRE, L. CUIEC, J. C. ROUSSEL and G. KASSAB, *J. Chim. Phys.* **92** (1995) 1885.
12. R. HANNUNIEMI, L. LAURÉN and H. PUOLIJOKI, *Drugs Today* **27** (1991) 375.
13. L. W. JELINSKI, in "Nuclear Magnetic Resonance in Modern Technology" edited by G. A. Maciel (Kluwer Academic Publishers, Netherlands, 1994) pp. 547–561.
14. W. M. RITCHEY, L. MAYLISH-KOGOVSEK and A. S. WALLNER, *Appl. Spectr. Rev.* **29** (1994) 233.
15. P. JEZZARD, J. J. ATTARD, T. A. CARPENTER and L. D. HALL, in "Progress in Nuclear Magnetic Resonance Spectroscopy" edited by J. W. Emsley, J. Feeney and L. H. Sutcliffe (Pergamon Press, Oxford, 1991) pp. 1–41.
16. R. A. KOMOROSKI, *Anal. Chem.* **65** (1993) 1068.
17. A. HAASE, J. FRAHM, D. MATTHAEI, W. HANICKE and K.-D. MERBOLDT, *J. Magn. Leson.* **67** (1986) 258.

Received 4 March

and Accepted 5 September 1997